A NEW PERSPECTIVE ON THE VERTICAL DISTRIBUTION OF DUST IN THE MARTIAN ATMOSPHERE IN NORTHERN SUMMER FROM MARS CLIMATE SOUNDER: ZONALLY-AVERAGED PROFILES. N.G. Heavens[1] M. I. Richardson[1], D.J. McCleese[2], A. Kleinböhl[2], and the MCS Science Team [1]Division of the Geological and Planetary Sciences, California Institute of Technology, MC 150-21, 1200 E. California Blvd., Pasadena, CA, 91125 (corresponding author: heavens@gps.caltech.edu) [2]Jet Propulsion Laboratory, California Institute of Technology, Pasadena, CA, 91109

Introduction: The distribution of dust with height in Mars' atmosphere is a critical unknown in the simulation of its general circulation and a source of insight into dust lifting, transport, and vertical mixing in the atmosphere. Consequently, observations of its optical properties and spatial and temporal variability have been a part of almost every major spacecraft mission sent to Mars. Unfortunately, the information provided by these missions about the vertical distribution of atmospheric dust has been limited. Limb retrievals of data from the Mars Climate Sounder (MCS) on Mars Reconnaissance Orbiter (MRO) are now greatly expanding our knowledge of vertical dust variability.

Recent measurements by the MCS (and in retrospect, limb observations by the Thermal Emission Spectrometer (TES) on Mars Global Surveyor (MGS) also show that middle atmospheric temperatures over the south pole during northern winter are > 10 K warmer than predicted by most Mars climate models for that relatively dust-free season, implying that most current models are underestimating the intensity of the Hadley circulation [1,2]. Basic considerations from simple nearly inviscid axisymmetric circulation models [3] and more sophisticated terrestrial models [4, 5] suggest that the Hadley circulation of a planet is sensitive to the vertical distribution of atmospheric heating.

Indeed, the distribution of dust in both the horizontal and the vertical affects both circulations to which polar warming could be attributed. It likely affects the intensity of the Hadley circulation through direct heating. But it also may affect the extratropical wave pump by stimulating waves through heating asymmetries and influencing wave propagation and dissipation by changing the stability profile of the atmosphere. Fortunately, vertical profiles of temperature, pressure, dust, and other aerosol retrieved from MCS observations now are providing an expansive dataset to investigate both the circulation and its potential forcings. Thus, knowledge of the vertical distribution of dust in the atmosphere provides a key constraint for Mars General Circulation Models (GCMs), analogous to the constraint cloud observations provide for terrestrial GCMs.

Because of the importance of the vertical dust distribution to these critical issues of the general circulation, this study will discuss zonally averaged profiles of the vertical variation of dust opacity from Mars as retrieved from observations by MCS, their novel features, and summarize their compact representation for purposes of analysis and prescribed dust forcings in meteorological models.

Methods: At present, atmospheric retrievals from Mars Climate Sounder observations (see *Kleinböhl et al.*, this meeting) provide vertical profiles of pressure (Pa), temperature (K), dust opacity, i.e., fractional extinction due to dust per unit height ($d_z\tau$), (km^{-1}) at 463 cm^{-1}, and water ice opacity (km^{-1}) at 842 cm^{-1}. The approximate ratio between the dust opacity at 463 cm^{-1} and visible dust opacity at 660 nm can be modeled to be ~4.3, and this ratio will be adopted for the purposes of this paper.

The retrievals are from a preliminary version of the standard Level 2 limb retrieval product delivered to the Planetary Data System, primarily differing from the released product in gridding, extrapolation, and post-processing as opposed to the retrieval algorithm. Thus the results of this study should be nearly reproducible from the standard product and the fitting scheme used in this study. One key element of this retrieval dataset is that information about dust from the detector observing the limb at ~8 km above the surface (detector 19 of channel A5) is used. The retrieval algorithm and post-processing also may bias sampling away from profiles over high topography or those that are especially dusty and icy. The key extrapolations are constant dust mass mixing assumptions at the top and the bottom of the profile. The former extrapolation is not necessary for the fitting scheme, but the latter is essential.

Vertical profiles of dust opacity were binned in 36 bins (5°) in latitude and 64 (5.625°) in longitude (2304 total) for each bin in L_s (5°) and local time (either between 21:00 and 9:00 LST or between 9:00 and 21:00 LST) during a period running from L_s=110°-165° in 2006-2007. These profiles were interpolated onto uniform grids in both pressure and sigma (σ) (the pressure ratioed by the surface pressure) and then averaged in their particular longitude, latitude, L_s bins before zonal averaging. Zonal average surface air densities, scale heights inferred from 5-20 km temperature-pressure data, and density-scaled opacities were calculated simi-

larly from the pressure and temperature retrievals. The impetus behind this particular averaging scheme was to ensure that while only the longitudes with valid retrievals would be sampled, each valid longitude contributed equally as opposed to the best-sampled longitudes biasing the results. Figure 1 shows sampling early in the period in the tropics is mainly restricted to the prime meridian on account of the equatorial cloud belt present during this season and sampling in the northern hemisphere is sparse as well.

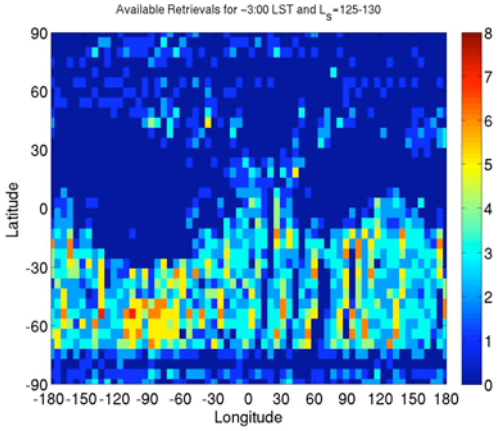

Figure 1: Number of samples in each spatial bin for morning (21:00 LST-9:00 LST retrievals) for L_s=125-130. Note that each latitude is generally sampled but only a small number of longitudes within that latitude.

A New Scheme for Representing Vertical Profiles of Dust Opacity: The Conrath scheme [6[is the conventional way to represent the vertical variation of dust in the martian atmosphere and has been used in GCMs, sometimes in a modified form. This scheme gives the functional form of the mass mixing ratio (q) as:

$$q = q_0 \exp\left[\nu(1-\sigma^{-1})\right] \qquad (1)$$

where q_0 is the mass mixing ratio of dust at the surface, ν is the ratio between the characteristic dust sedimentation and atmospheric diffusion times of the atmosphere at the surface, and σ the ratio between the ambient pressure and the surface pressure. One key advantage of this scheme is that it simplifies the problem of the vertical dust distribution to two physical processes of some complexity (sedimentation and diffusion) in a quantitatively elegant way.

To demonstrate the problems encountered when using the Conrath scheme to represent MCS dust profiles, let us simplify dust aerosol to be composed of particles of uniform size, shape, and composition and claim that since (at fixed wavelength):

$$d_z\tau = Q_{ext} N \pi r^2 \qquad (2)$$

where Q_{ext} is the extinction coefficient, N is the number density of particles, and r is the effective radius, then:

$$\frac{d_z\tau}{\rho} = \frac{Q_{ext}\pi r^2}{m_d} q \qquad (3)$$

$d_z\tau$ is the opacity scaled by the air density and m_d is the mass of an individual dust particle. Thus, the density-scaled opacity should be roughly proportional to the mass mixing ratio and in the optically thin case, also proportional to the heating/cooling rate due to dust.

Figure 2 shows an example of the zonal average of density-scaled opacities from MCS retrievals and the zonal average of density-scaled opacity for the observed pressure and temperature conditions that would be used to force the MGS scenario of the Mars Climate Database [7,8] scaled by the modeled ratio between visible and 463 cm^{-1} opacity. This scenario uses a modified Conrath profile.

The crucial difference between the MCS dust-scaled opacities and what might be expected from a Conrath profile is the elevated maximum in density-scaled opacity over the tropics. The Conrath profile cannot account for such an extremum. The small density-scaled opacities seen near the top are due to the constant mass mixing ratio assumption at the top of the profiles and should be ignored. The elevated maximum in density-scaled opacity above the south pole may be due to an unretrieved aerosol, carbon dioxide, and likewise should be ignored.

An empirical scheme has been developed, which fits the dust opacities as a product of σ (vertical coordinate) and a function involving two gaussians. The first gaussian represents the decay from constant mass mixing ratio near the surface and is truncated by means of a Heaviside function, while the second represents structures like the elevated maximum in the tropics ("the pulse"). Figure 3 shows examples of these fits.

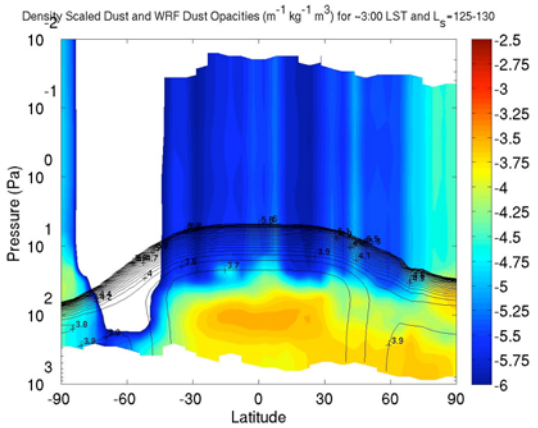

Figure 2: Zonally averaged density-scaled opacity interpolated onto pressure coordinates for L_s=125-130 at ~3:00 LST: (colors) from MCS retrievals; (labeled contours) based on the Martian Year 24 MGS dust scenario in the Mars Climate Database with MCS retrieval pressure and temperature information.

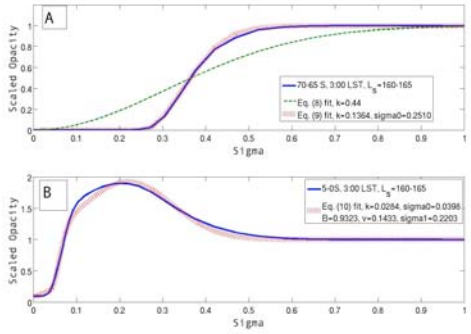

Figure 3: (a) Example "unperturbed" scaled opacity profile fit with gaussian decay from constant mass mixing ratio, truncated by means of a Heaviside function. The green curve shows an early unsuccessful attempt at the fit, which ignored the truncation. (b) example "perturbed" scaled opacity profile fit with gaussian decay from constant mass mixing ratio, delimited by a Heaviside function and a gaussian to represent an elevated pulse in mass mixing ratio.

Variations in Dust Concentration and Vertical Mixing during L_s=110-165:

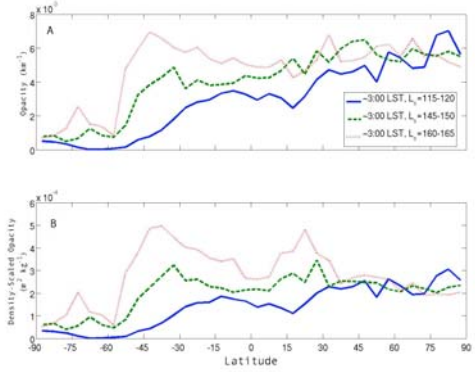

Figure 4: (a) Inferred near-surface dust opacity (km^{-1}) vs. latitude for zonally-averaged opacity profiles at ~3:00 LST for various L_s bins showing changes in boundary layer "dustiness" over the season (b) Inferred near-surface density-scaled opacity (m^2 kg^{-1}) vs. latitude for zonally-averaged opacity profiles at ~3:00 LST for the L_s bins used in (a), showing changes in the approximate boundary layer mass mixing ratio as the northern autumnal equinox approaches. Note the significant increase in dustiness ~ 45°S during the period.

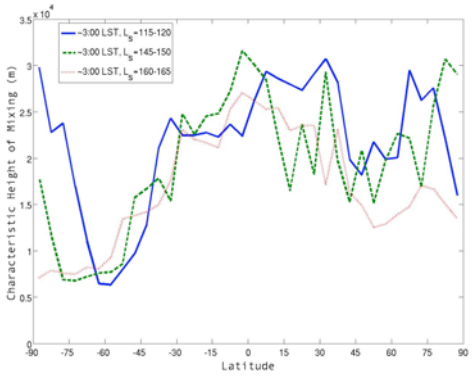

Figure 5: Height (m) at which density-scaled opacity is 1/e of its near-surface value (excluding the pulse) vs. latitude for zonal averages at ~3:00 LST for various L_s bins showing latitudinal changes in vertical dust mixing with season. Note the increasing clearing in the northern extratropics and more poleward clearing in the south during this period.

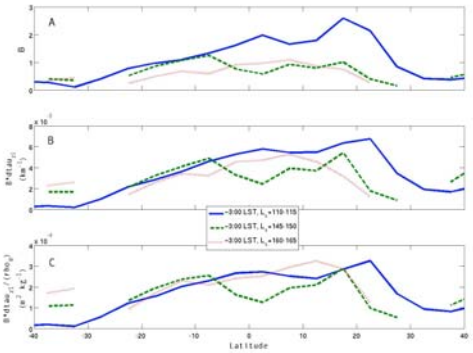

Figure 6: (a) Relative magnitude of the pulse (B) vs. latitude for zonally-averaged opacity profiles at ~3:00 LST for various L_s bins, showing apparent change during late northern summer; (b) Absolute magnitude of the pulse (km^{-1}) vs. latitude for zonally-averaged opacity profiles at ~3:00 LST for the L_s bins used in (a), implying less variation in the absolute magnitude of the pulse in scaled opacity above the equatorial boundary layer during northern summer than implied by (a); (c) Density-scaled opacity due to the pulse (m^2 kg^{-1}) vs. latitude for zonally-averaged opacity profiles at ~3:00 LST for the L_s bins used in (a) and (b), which is an approximate metric of the relative effect of the pulse on heating and cooling rates.

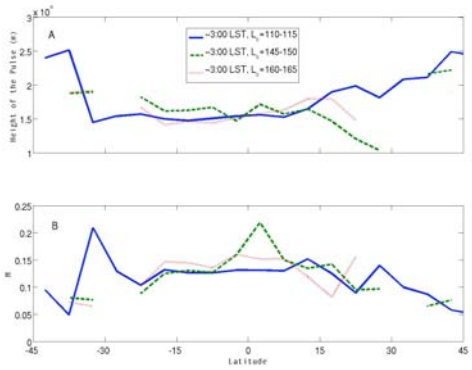

Figure 7: (a) Height (m) of the maximum density-scaled opacity due to the pulse vs. latitude inferred from zonal averages at ~3:00 LST for various L_s bins; (b) Parameter governing the width of the pulse inferred from zonal averages at ~3:00 LST for various L_s bins. These values indicate the pulse is ~5-10 km wide.

A Preview of MCS Dust Scenarios: Two prescribed dust forcing schemes have been developed in order to test possible ways to incorporate the new information about vertical dust opacity variations from MCS into meteorological models. The first scheme uses the results of the empirical fitting scheme to provide the vertical profile but uses the optical depth functions of the MGS dust scenario of the Mars Climate Database to specify the total optical depth in each profile, because of doubts whether dust is sufficiently well-mixed with height to justify a constant extrapolation of dust mass mixing ratio from ~8 km to the surface. An example of the output of this scheme (for comparison with Figure 2) is shown in Figure 8. The second scheme (Figure 9) assumes dust is sufficiently well-mixed that the constant mass mixing ratio extrapolation is approximately correct and both the absolute MCS dust opacities and their vertical variation are used to derive the second scheme. The representation of the pulse proves problematic for both schemes, introducing a tail of overly high mass mixing ratio at height. This problem can be eliminated by bounding the vertical extent of dust, either using the commonly used function due to *Jaquin et al.* [9] or the Heaviside truncation parameter, σ_0, used in our fitting scheme.

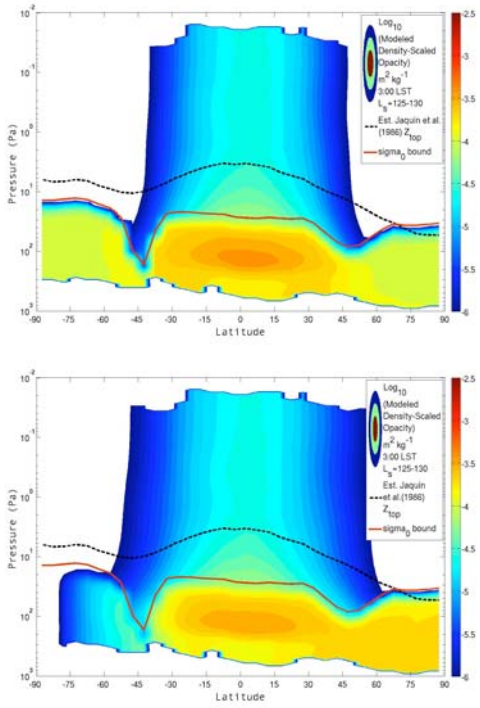

Figures 8 and 9: Zonally averaged density-scaled opacity based on the MCS prescribed dust schemes described (top: uses MGS dust scenario of Mars Climate Database total column opacity function; bottom: all opacity information from MCS) projected onto pressure coordinates for L_s=125-130 with lines showing possible cut-off criteria for the tail of the "pulse."

Summary: Dust opacity profiles in MCS limb retrievals during northern summer provide a higher resolution picture in time, vertical, and horizontal space of atmospheric dust variability than ever before. Zonally-averaged profiles show seasonal variation in the depth of mixing throughout the atmosphere, but imply the existence of a persistent region of elevated mass mixing ratio at ~10-20 km altitude in the tropics, "the pulse." Aspects of the pulse will be investigated by *Heavens et al.* (this meeting).

References: [1] M.D. Smith *et al.* (2001), *JGR*, **106**, 23929-23945; [2] D.J. McCleese et al., *Nature Geosci.*, in press; [3] E.K. Schneider (1983), *Icarus*, **35**, 302-331; [4] D. Rind and W.B. Rossow (1984), *JAS*, **41** (4), 479-507; [5] J. Wang and W.B. Rossow (1998), *J. Climate*, **11**, 3010-3029; [6] B.J. Conrath (1975), *Icarus*, **24**, 36-46. [7] F. Forget *et al.* (1999), *JGR*, *104*, 24155–24175. [8] S.R. Lewis *et al.* (1999), *JGR*, **104**, 24177-24194; [9] F. Jaquin *et al.* (1986), *Icarus*, **72**, 528-534.